JACC: ADVANCES VOL. 2, NO. 7, 2023

ORIGINAL RESEARCH

EMERGING TECHNOLOGIES AND INNOVATIONS

Accuracy of IVUS-Based Machine Learning Segmentation Assessment of Coronary Artery Dimensions and Balloon Sizing

Mitsuaki Matsumura, BS,[a,b] Gary S. Mintz, MD,[a] Tomotaka Dohi, MD, PhD,[b] Wenguang Li, PhD,[c] Alexander Shang, BSE,[c] Khady Fall, MD, MPH,[d] Takao Sato, MD,[a,d] Yoichiro Sugizaki, MD,[a,d] Yiannis S. Chatzizisis, MD,[e] Jeffery W. Moses, MD,[a,d] Ajay J. Kirtane, MD, SM,[a,d] Hajime Sakamoto, PhD,[f] Hiroyuki Daida, MD, PhD,[f] Tohru Minamino, MD, PhD,[b] Akiko Maehara, MD[a,d]

ABSTRACT

BACKGROUND Accurate intravascular ultrasound (IVUS) measurements are important in IVUS-guided percutaneous coronary intervention optimization by choosing the appropriate device size and confirming stent expansion.

OBJECTIVES The purpose of this study was to assess the accuracy of machine learning (ML) automatic segmentation of coronary artery vessel and lumen dimensions and balloon sizing.

METHODS Using expert analysis as the gold standard, ML segmentation of 60 MHz IVUS images was developed using 8,076 IVUS cross-sectional images from 234 patients, which were randomly split into training (83%) and validation (17%) data sets. The performance of ML segmentation was then evaluated using an independent test data set (437 images from 92 patients). The endpoints were the agreement rate between ML vs experts' measurements for appropriate balloon size selection, and lumen and acute stent areas. Appropriate balloon size was determined by rounding down from the mean vessel diameter or rounding up from the mean lumen diameter to the next balloon size. The difference of lumen area $\geq$0.5 mm^2 was considered as clinically significant.

RESULTS ML model segmentation correlated well with experts' segmentation for training data set with a correlation coefficient of 0.992 and 0.993 for lumen and vessel areas, respectively. The agreement rate in lumen and acute stent areas was 85.5% and 97.0%, respectively. The agreement rate for appropriate balloon size selection was 70.6% by vessel diameter only and 92.4% by adding lumen diameter.

CONCLUSIONS ML model IVUS segmentation measurements were well-correlated with those of experts and selected an appropriate balloon size in more than 90% of images. (JACC Adv 2023;2:100564) © 2023 The Authors. Published by Elsevier on behalf of the American College of Cardiology Foundation. This is an open access article under the CC BY-NC-ND license (http://creativecommons.org/licenses/by-nc-nd/4.0/).

From the [a]Clinical Trial Center, Cardiovascular Research Foundation, New York, New York, USA; [b]Department of Cardiovascular Medicine, Juntendo University Graduate School of Medicine, Tokyo, Japan; [c]Boston Scientific Corporation, Maple Grove, Minnesota, USA; [d]NewYork-Presbyterian Hospital, Columbia University Irving Medical Center, New York, New York, USA; [e]Cardiovascular Division, University of Nebraska Medical Center, Omaha, Nebraska, USA; and the [f]Department of Radiology Technology, Juntendo University Faculty of Health Science, Tokyo, Japan.

Manuscript received February 8, 2023; revised manuscript received May 18, 2023, accepted June 13, 2023.

ISSN 2772-963X https://doi.org/10.1016/j.jacadv.2023.100564

ABBREVIATIONS AND ACRONYMS

AI = artificial intelligence

CNN = convolution neural network

DES = drug-eluting stent(s)

DSC = dice similarity coefficient

IoU = intersection over union

IVUS = intravascular ultrasound

ML = machine learning

PCI = percutaneous coronary intervention

Intravascular ultrasound (IVUS) is used to guide percutaneous coronary intervention (PCI) in treating coronary artery disease,[1,2] and IVUS guidance has improved patient outcomes in both short- and long-term follow-up compared with angiography alone.[3-7] The 2021 American Heart Association/American College of Cardiology and Society of Cardiovascular Angiography and Interventions Guideline for Coronary Artery Revascularization and the 2018 guidelines from the European Society of Cardiology give a Class 2a recommendation for IVUS guidance in patients undergoing coronary stent implantation.[8,9] However, the real-world usage of IVUS guidance remains low despite its benefits.[10,11] One possible reason is the lack of physician education leading to misinterpretation of IVUS images.[12] IVUS measurements must be accurate in the clinical setting.

The medical field is taking advantage of artificial intelligence (AI) technology with regard to diagnostic imaging interpretation. We hypothesized that intravascular imaging could also benefit from AI. Fully automatic assessment of vessel geometry such as lumen, vessel wall, and plaque burden using IVUS should greatly facilitate diagnosis and treatment planning by reducing the time and effort needed to manually obtain key measurements. Several image segmentation technologies based on traditional filter design and pattern recognition for automatic IVUS image segmentation have been developed over the decades, but with limited success and/or adoption.[13]

Recent advancements in deep machine learning (ML) technologies with convolution neural networks (CNNs) have provided a potential solution to this challenge.[14-17] The key difference between the new CNN and traditional pattern recognition is the increase in the "depth" of the network, providing millions of parameters that can be trained to match the input with desired output to mimic the capability of an expert. This study aimed to assess the accuracy of ML automatic segmentation of coronary artery vessel and lumen dimensions and balloon sizing using high-definition (HD) IVUS images.

METHODS

STUDY DATA SET. Two separate data sets were prespecified. The first data set was used for training and validation, and the second data set was used for independent testing. All IVUS images were taken using the HD 60 MHz IVUS OptiCross IVUS catheter paired with the iLab Polaris Multi-Modality Guidance System (Boston Scientific Corporation). IVUS was performed in a standard manner using an automated transducer pullback at 0.5 or 1.0 mm/s with a 40 mm or longer pullback length. The first data set included 8,076 IVUS cross-sectional images from 234 patients located in Asia, Europe, or the United States; and the second data set included 437 cross-sectional images from 92 patients from the United States. Of note, images from each institution including U.S. sites were included in either the first or second data set, but not both. The Institutional Review Board of all sites approved the study protocol and patient consent was waived due to minimal risk.

IVUS IMAGE ANALYSIS. In both the first and second data sets, the lumen or stent and vessel areas were analyzed by experts using a preloaded Polaris simulator. In the first data set, the analysis was done for the entire vessel; whereas in the second data set, the analysis was done at the minimum lumen area site, minimum stent area site if stented, and proximal and distal reference sites. Proximal and distal reference sites were the least plaque burden within 5 mm of the edge of the lesion but before any major side branch ($>$1.5 mm in diameter). Mean lumen and vessel diameters were calculated from the lumen or vessel area.

IVUS U-NET MODEL DEVELOPMENT. The ML segmentation algorithm was trained using expert analysis as the gold standard. In the first data set, the training data set (83% of images) and validation data set (17% of images) were randomly selected; and the IVUS images from one patient were either in the training or validation data set, but not both. In addition, image argumentation techniques were applied to eliminate the effect from IVUS image variations such as brightness and the orientation of an IVUS cross-section image.

Among various types of CNNs, the "U-Net" has been one of the most successful ML architectures for biomedical image segmentation. An example of U-Net lumen segmentation has been shown in Figure 1. The input for the model was a resized IVUS image as a contractive path, which is to enhance the object of interest by losing other details while the output of the model was the mask image as an expansive path to create vessel, lumen, and stent areas separately with a high-resolution segmentation map. In the end, the output segmentation masks had the same resolution as the input image. Representative images have been shown in Figure 2.

PRIMARY ENDPOINT. The primary endpoint was the agreement rate of appropriate balloon size selection between ML vs expert analysis at the individual slice

FIGURE 1 **U-Net Lumen Segmentation Example**

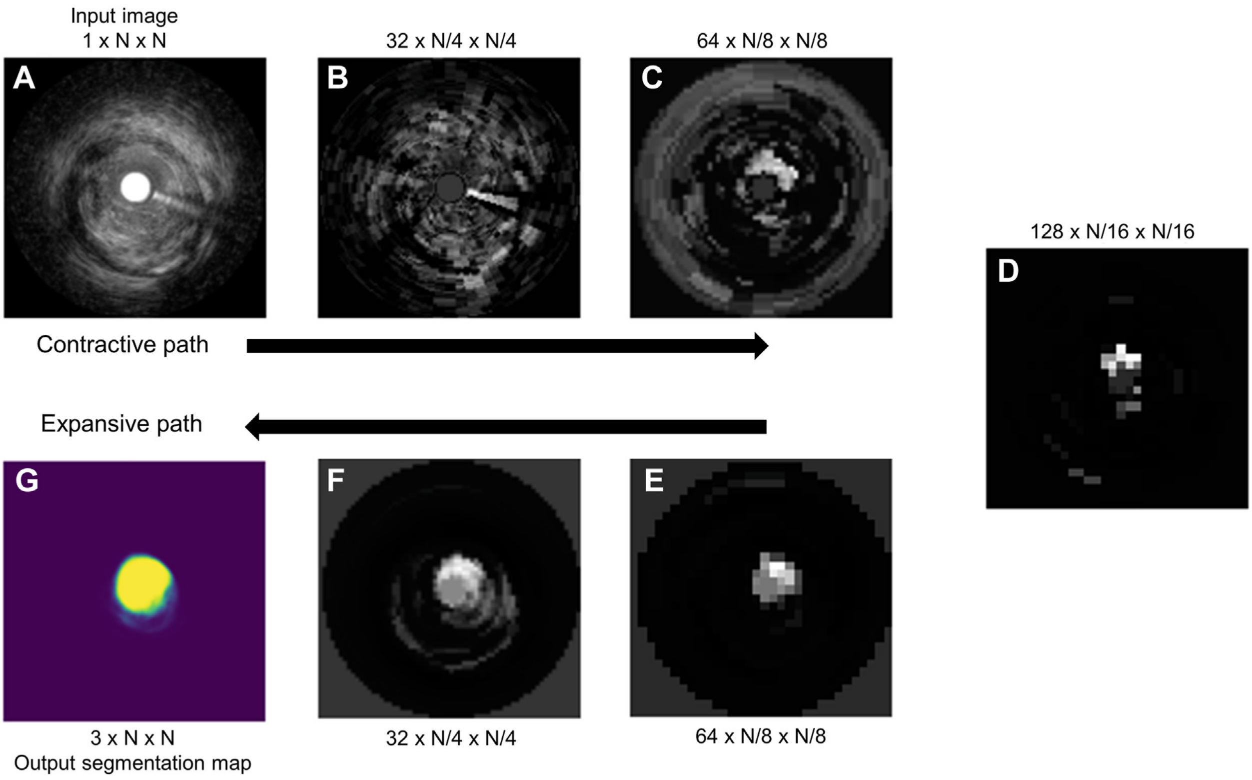

Upper images (A to D) show the contractive path from input image, and **lower images (E to G)** show expansive path to output segmentation map - first into an increasing number of lower-resolution features along the contractive path **(A to D)**, and then into a decreasing number of higher-resolution features along the expansive path **(D to G)**. At each level, one of many features was arbitrarily chosen and transformed to cartesian coordinates for ease in interpretability.

level in an independent data set. First, the appropriate balloon size was determined by rounding *down* from the mean *vessel* diameter to the next balloon size. If the ML chosen balloon size was different from the expert, the appropriate balloon size was then determined by rounding *up* from the mean *lumen* diameter to the next balloon size.[18] The endpoint was repeated at the lesion level.

Because the post-PCI absolute lumen or stent area is the most powerful parameter to be associated with the long-term outcome, we set the secondary endpoint as the agreement rate in lumen area between ML vs expert analysis using a difference of <0.5 mm^2 as an acceptable cutoff in IVUS frames having lumen area <9.0 mm^2.[19,20] In other words, a difference of ≥ 0.5 mm^2 in lumen area measurement was considered as clinically significant in a ≤ 3.5 mm angiographic vessel. In addition, the agreement rate in the acute stent area was assessed using the same acceptable cutoff used for the lumen area. As an exploratory analysis, we evaluate interobserver variability of lumen and vessel area measurements between 2 interventional cardiologists and compared them with those obtained between ML and expert analysis.

STATISTICAL ANALYSIS. The primary and secondary endpoints were descriptive and shown as the rate of agreement between ML vs expert analysis. The metrics used for the evaluation were the mean intersection over union (IoU) and dice similarity coefficient (DSC), common evaluation metrics for semantic image segmentation, which first computed the IoU and DSC for each semantic class and then computed the average over classes. IoU and DSC were defined as follows:

IoU = true positives/(true positives + false positives + false negatives)

DSC = 2 × true positives/(2 × true positives + false positives + false negatives)

To assess the practical validity, the agreement and correlation of the lumen, vessel, and stent areas between the ML model segmentation and the

FIGURE 2 **Representative Images**

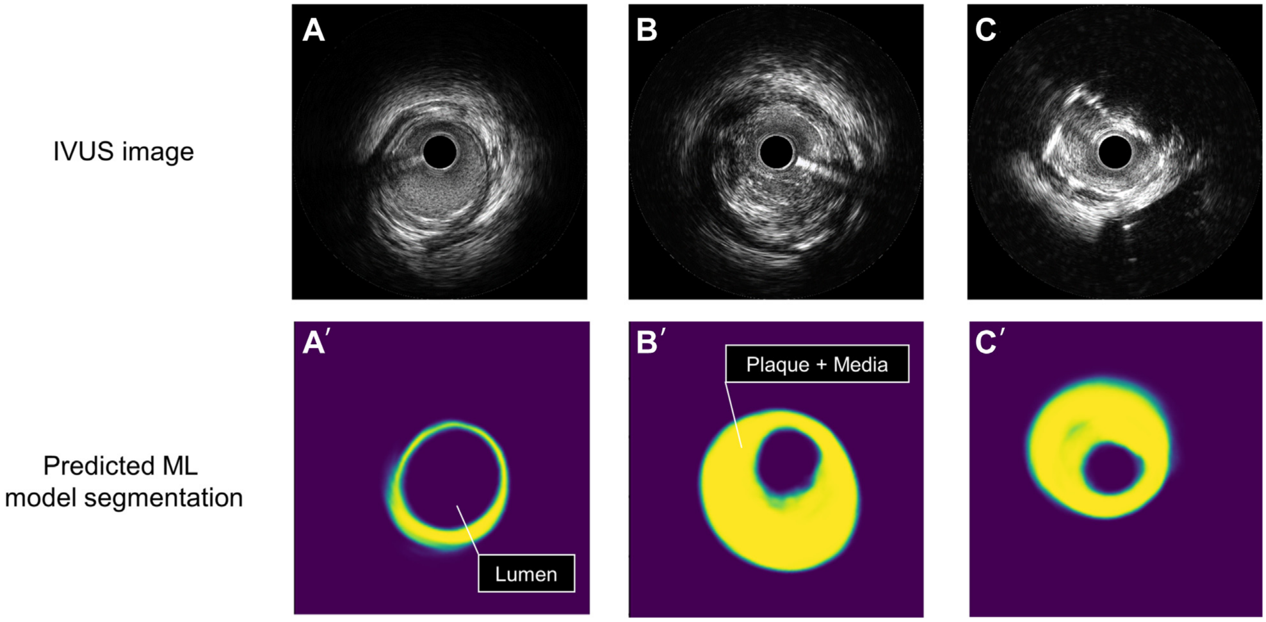

(A) IVUS image with visible vessel border ≥270°, **(A′)** predicted machine learning (ML) model segmentation corresponding to IVUS image A. **(B)** IVUS image with visible vessel border 180° to 270°, **(B′)** predicted ML model segmentation corresponding to IVUS image B. **(C)** IVUS image with visible vessel border <180°, **(C′)** predicted ML model segmentation corresponding to IVUS image C. **Purple color** in the most inside in figures **(A′ to C′)** shows predicted ML lumen area; and **yellow color** shows plaque+media area. IVUS = intravascular ultrasound; ML = machine learning.

expert analysis were assessed by Pearson correlation coefficient, and mean differences were visualized by scatter and Bland-Altman plots. Continuous variables were expressed as mean ± SD or 95% CI. Interobserver variability of lumen and vessel areas was tested between ML analysis vs expert analysis, and between 2 interventional cardiologists in 40 randomly selected IVUS images using an intraclass correlation coefficient. A P value <0.05 was considered to indicate statistical significance. The statistical analyses were performed using EZR statistics version 4.0.2 (R Foundation for Statistical Computing).

TABLE 1 **Performance of the Machine Learning-Based Segmentation Against Observers on the Training and Validation Set**

	Overall (N = 8,076)	Training (n = 6,669)	Validation (n = 1,407)
Lumen area			
Intersection over union	0.92 ± 0.05	0.92 ± 0.05	0.91 ± 0.06
Dice similarity coefficient	0.96 ± 0.03	0.96 ± 0.03	0.95 ± 0.03
Correlation coefficient	0.991 (0.991-0.991)	0.992 (0.991-0.992)	0.984 (0.983-0.986)
Mean difference	−0.08 ± 0.52	−0.09 ± 0.51	−0.05 ± 0.56
Vessel area			
Intersection over union	0.94 ± 0.04	0.94 ± 0.04	0.93 ± 0.06
Dice similarity coefficient	0.97 ± 0.02	0.97 ± 0.02	0.96 ± 0.03
Correlation coefficient	0.991 (0.991-0.991)	0.993 (0.993-0.994)	0.976 (0.974-0.979)
Mean difference	−0.11 ± 0.88	−0.12 ± 0.78	−0.02 ± 1.26

Values are mean ± SD or mean (95% CI).

RESULTS

ACCURACY OF IVUS-BASED ML SEGMENTATION. In the first data set used for training and validation (n = 8,076), the mean areas of the lumen and vessel were 7.5 ± 3.9 mm^2 and 15.2 ± 6.6 mm^2, respectively. The diagnostic performance of the ML model segmentation has been summarized in Table 1. The ML model segmentation correlated well with expert segmentation for the training data set with a mean IoU of 0.92 ± 0.05 and 0.94 ± 0.04, correlation coefficients of 0.992 (95% CI: 0.991-0.992) and 0.993 (95% CI: 0.993-0.994), and mean differences of −0.09 ± 0.51 mm^2 and −0.12 ± 0.78 mm^2 for lumen and vessel areas, respectively (Table 1).

A total of 437 IVUS images in 92 patients were labeled by expert analysis in an independent data set. Of 437 IVUS images, 42 images (9.6%) were within the stent, of which 33 images had new stents; and 395 (90.4%) were in a non-stented segment. The mean areas of the lumen and vessel were 6.8 ± 4.0 mm^2 and 12.7 ± 5.8 mm^2, respectively. A strong correlation of the lumen area was found between the ML model segmentation and the expert analysis with a mean difference of −0.10 ± 0.54 (correlation coefficient: 0.991 [95% CI: 0.989-0.993], $P < 0.001$) (**Table 2**, **Figures 3A and 3B**). Similarly, a strong correlation of the vessel area was found between the ML model segmentation and the expert analysis with a mean difference of 0.29 ± 1.47 (correlation coefficient: 0.967 [95% CI: 0.960-0.973], $P < 0.001$) (**Table 2**, **Figures 3C and 3D**). When the vessel area was categorized into 3 groups stratified by visible vessel border, the images having a larger visible vessel border (≥270°) had less difference when compared to those having a less visible vessel border (<180°) (mean: −0.02 ± 0.50 vs 0.75 ± 2.59, $P = 0.02$) (**Figure 4**).

There was a similarly good intraclass correlation coefficient for measurements of lumen and vessel areas between ML and expert analysis (95% CI: 0.998-0.993) and between 2 interventional cardiologists (95% CI: 0.996-0.996), respectively. The mean difference of lumen area between ML and expert and between 2 cardiologists was −0.04 ± 0.43 and −0.13 ± 0.55, respectively ($P = 0.47$). The mean difference of vessel area was 0.01 ± 1.03 and 0.29 ± 0.86, respectively ($P = 0.13$) (Supplemental Figure 1).

PRIMARY AND SECONDARY ENDPOINT. The primary endpoint was the agreement rate of appropriate balloon size selection between ML vs expert analysis in an independent data set. Using mean vessel diameter, the rate of agreement was 70.6%, and adding mean lumen diameter, the overall rate of agreement was 92.4% (primary endpoint) (**Figure 5**, **Central Illustration**). If only images with visible vessel border <180° were applied, it was 45.5%, if only images with visible vessel border ≥180° and <270° were applied, it improved to 68.9%; and if only images with visible vessel border ≥270° were applied, it was further improved to 80.7%. By adding the assessment of mean lumen diameter, the rate of appropriate balloon size chosen by ML was improved to 85.2% in visible vessel border <180°, 91.9% in visible vessel border ≥180° and <270°, and 95.3% in visible vessel border ≥270°.

Because balloons and stents come in 0.25 mm sizes, differences in diameter measurements <0.25 mm could be considered as acceptable. When a difference of 0.25 mm in the lumen and/or vessel diameters was considered as a cutoff value, 94.4% of the lumen and 88.9% of vessel diameters were within ±0.25 mm difference (**Figure 6**). When only images with visible vessel border ≥270° were included, 97.9% of the images were with ±0.25 mm difference; when images with visible vessel border ≥180° and <270° were included, 89.2% had a ±0.25 mm difference; and when images with visible vessel border <180° were included, 63.6% had a ±0.25 mm difference (Supplemental Figure 2). The prevalence of ≥0.5 mm of larger balloon size was observed in 5.3%, which was mostly found in the images with visible vessel borders <180°. Using multivariable linear regression to predict the errors of balloon sizing including the presence of myocardial bridge, vessel diameter by expert, vessel location in left anterior descending, and vessel visibility, vessel visibility was independently associated with the errors of balloon sizing (**Table 3**).

TABLE 2 **Correlation Between Machine Learning and Expert Analysis in an Independent Data Set**

	Correlation Coefficient	95% CI	*P* Value	Mean Difference	SD
At slice level (n = 437)					
Lumen area	0.991	0.989-0.993	<0.001	−0.10	0.54
Vessel area	0.967	0.960-0.973	<0.001	0.29	1.47
Stent area	0.982	0.966-0.990	<0.001	0.05	0.46
Mean lumen diameter	0.985	0.981-0.987	<0.001	−0.01	0.13
Mean vessel diameter	0.965	0.958-0.972	<0.001	0.06	0.23
At lesion level (n = 92)					
Lumen area	0.994	0.990-0.996	<0.001	−0.20	0.41
Vessel area	0.987	0.981-0.992	<0.001	0.18	0.81
Mean lumen diameter	0.986	0.979-0.991	<0.001	−0.03	0.10
Mean vessel diameter	0.982	0.973-0.988	<0.001	0.04	0.15

The secondary endpoint was an 85.5% agreement rate in lumen area between ML vs expert analysis using a difference of <0.5 mm^2[19,20] as an acceptable cutoff difference in lesions with lumen area ≤9.0 mm^2 (**Figure 7**). When 5% difference of lumen area was applied for all lumen areas, 76.2% were in agreement; and when lumen area difference <0.5 mm^2 or 5% difference of lumen area was applied, 86.3% were in agreement. There were only 33 images with new stents. When the acute stent area was compared between ML vs expert analysis using a difference of <0.5 mm^2 as a cutoff, the agreement rate was 97.0% (**Central Illustration**).

LESION LEVEL ANALYSIS. When we consider the clinical setting, the balloon sizing should be done based on the distal reference vessel diameter first,

FIGURE 3 **Comparison of Lumen and Vessel Areas Between Expert Analysis and Machine Learning Model Segmentation**

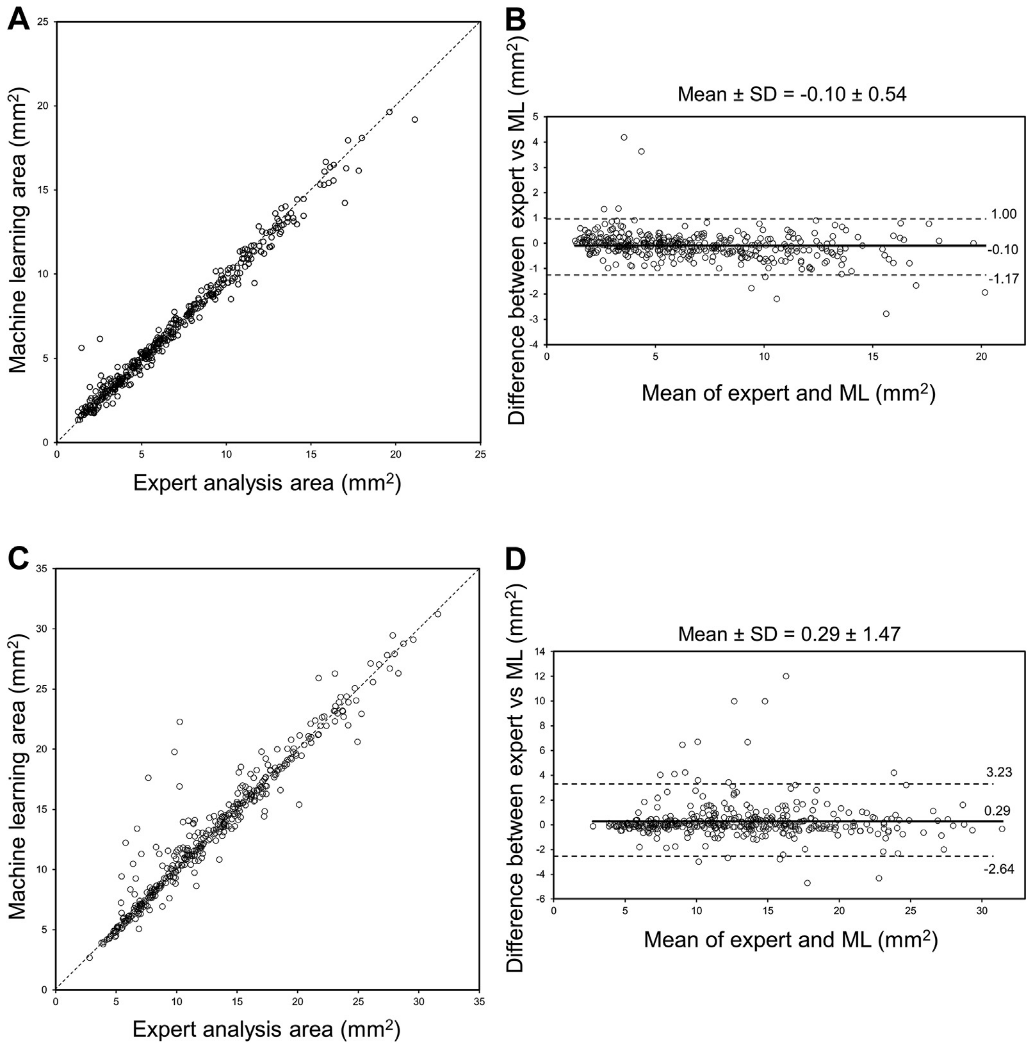

(A) Correlation of lumen area. **(B)** Bland-Altman plot of lumen area. Mean difference is shown in **solid line** and ±2 SD of the difference are shown in **dotted lines**. **(C)** Correlation of vessel area. **(D)** Bland-Altman plot of vessel area. Mean difference is shown in **solid line** and ±2 SD of the difference are shown in **dotted lines**. Abbreviation as in Figure 2.

and then lumen diameter if visible vessel border <180°. If distal reference is not available, either proximal reference or minimum lumen area sites should be chosen. When we applied this algorithm to the most representative 92 lesions in 92 patients (ie, one lesion per patient), the agreement rate of balloon or stent sizing was 76.1% by using mean vessel diameter and 91.3% by using both vessel and lumen diameters. Lesion level correlation between ML and expert analysis is consistent with slice level analysis (**Table 2**, Supplemental Figure 3). Moreover, when we calculate the rate of the different sizing when using distal or proximal references or the minimum lumen area site in the same lesion, more than 90% of the lesions had different sizing depending on the anatomic location chosen.

DISCUSSION

The main findings of this study were that the ML model segmentation of lumen, vessel, and stent areas was strongly correlated with those obtained by manually labeled segmentation. Better visibility of vessel border was associated with more accurate

FIGURE 4 **Correlation Between Expert Analysis and Machine Learning Model Segmentation of Vessel Area Stratified by Visible Vessel Border**

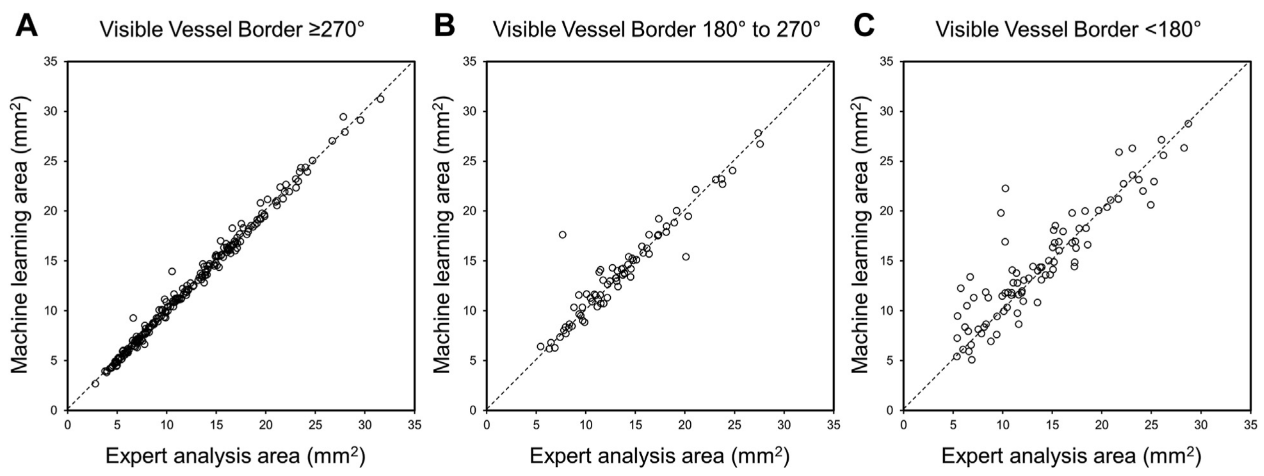

(A) Visible vessel border ≥270°, **(B)** visible vessel border 180° to 270°, **(C)** visible vessel border <180°.

measurements of vessel area by ML model segmentation. Overall, appropriate balloon size was chosen in more than 90% of images by combining vessel and lumen ML measurements. Acceptable lumen and acute stent measurements were seen in more than 85% and 95% of images. The similar levels of SD for both lumen and vessel areas between ML and expert and between 2 cardiologists indicated the capability of the ML model was approaching to that of a cardiologist.

Recent developments in AI have improved an automated, objective, and quantitative approach to

FIGURE 5 **The Prevalence of Appropriate Balloon Size Chosen Stratified by Visible Vessel Diameter**

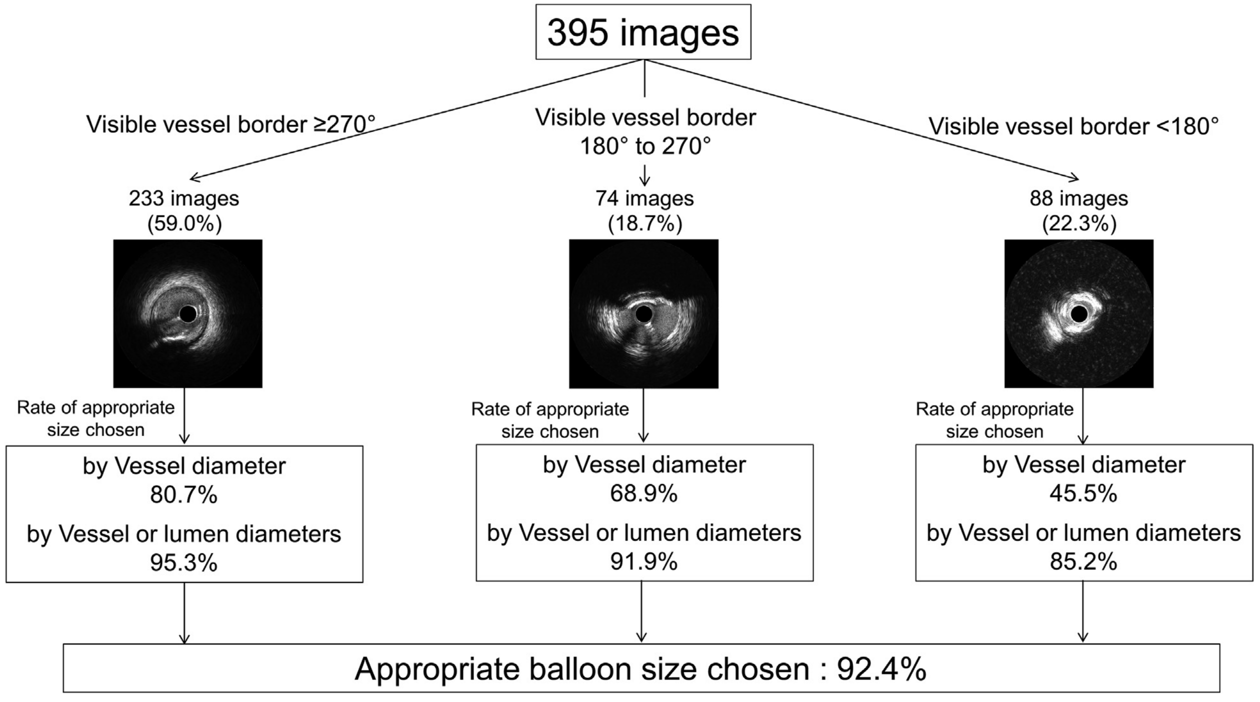

CENTRAL ILLUSTRATION **The Agreement Rate for Appropriate Balloon Size Selection, and Lumen and Acute Stent Areas**

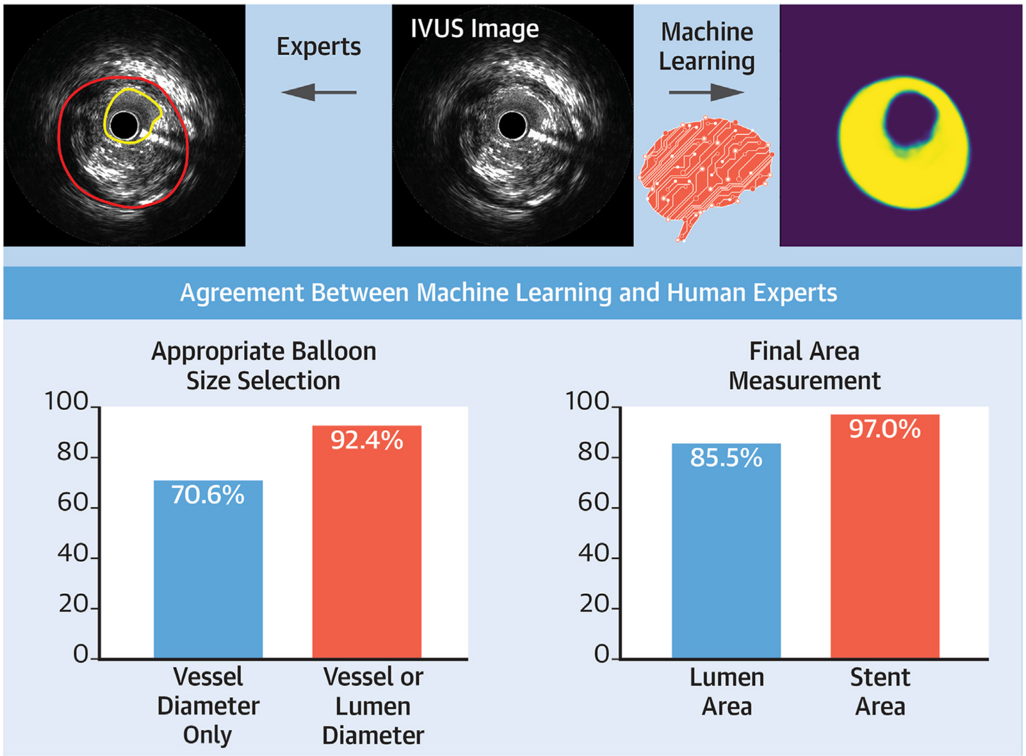

Matsumura M, et al. JACC Adv. 2023;2(7):100564.

The agreement rate for appropriate balloon size selection was 70.6% by vessel diameter only and 92.4% by adding lumen diameter. The agreement rate in lumen and acute stent areas was 85.5% and 97.0%, respectively. IVUS = intravascular ultrasound.

evaluating vessel dimensions with IVUS.[14] Deep learning methods have been proposed to develop automated IVUS segmentation.[21,22] Recent advancements of deep ML technologies with CNN have achieved relatively high performance for the segmentation of the lumen and vessel areas.[15,23] Yang et al[15] demonstrated that the IoU of vessel and lumen in the test data set was 0.86 and 0.90 using 20 MHz IVUS from 10 patients. Another study that used a full CNN with encoder/decoder networks with the main body being DeepLabv3 demonstrated that the mean IoU in the test data set was 0.88 using 40 to 45 MHz IVUS from 1,850 images.[23] Thus, ML measurements by HD IVUS suggested more accurate detection of lumen and vessel areas.

In the drug-eluting stent (DES) era, intravascular imaging-guided stent or post-stent balloon sizing recommendations have been based on either: 1) vessel diameters of the proximal reference, distal reference, or lesion site, usually rounded down by 0.25 mm; or 2) rounded up from the mean lumen diameter[18] or by averaging the media-to-media diameters of the proximal and distal stent segments, as well as at the sites of maximal narrowing within the stent, and the value was rounded to the lower 0.00 or 0.50 mm.[24] Conversely, when lumen diameter was used, the expert consensus of the European Association of PCI suggested that a mean distal lumen reference-based sizing with rounding up by 0 to 0.25 mm may represent a safe and straightforward approach with subsequent optimization of the mid and proximal stent segments.[9] It should be noted that about 15% of lesions may have negative remodeling with less plaque such that stent and/or balloon sizing by ML model segmentation considering not only vessel diameter but also lumen diameter could be more appropriate.[25]

FIGURE 6 **The Difference of Lumen and Vessel Diameters Between Expert and Machine Learning Model Segmentation**

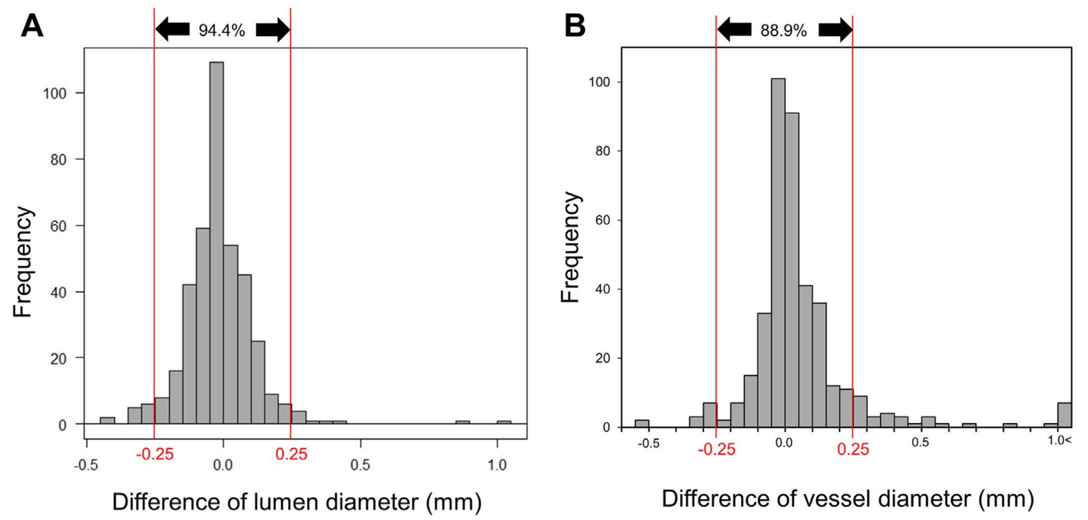

(A) Difference of lumen diameter, **(B)** difference of vessel diameter.

Numerous prior IVUS studies have reported that absolute minimum stent area, which is clinically the same meaning as minimum lumen area in the stented segment, is the most powerful predictor of clinical events, even in the contemporary DES era.[26,27] Meta-analyses of randomized trials and registry data have shown significant major adverse cardiovascular event reductions with IVUS-guided PCI compared with angiography-guided PCI.[28-30] The IVUS-XPL (Impact of Intravascular Ultrasound Guidance on the Outcomes of Xience Prime Stents in Long Lesions) study demonstrated that major adverse cardiovascular event reductions were significant with a hazard ratio of 0.50 (95% CI: 0.34-0.75) in the IVUS-guided cohort compared with the angiography-guided cohort at 5-year follow-up.[7] In the ULTIMATE (Intravascular Ultrasound Guided Drug Eluting Stents Implantation in “All-Comers” Coronary Lesions) study, which used minimum lumen area in the stented segment as one of the optimal criteria, target vessel failure occurred in 47 patients (6.6%) in the IVUS-guided group and 76 patients (10.7%) in the angiography-guided group ($P = 0.01$), driven mainly by the decrease in clinically driven target vessel revascularization (4.5% vs 6.9%; $P = 0.05$) at 3-year follow-up.[6] IVUS-guided DES implantation improves outcomes because of a significantly larger minimum stent area and minimum lumen diameter compared to angiography-guided PCI.[5,18] Therefore, IVUS was beneficial in clinical settings not only for acute larger stent areas but also for long-term outcomes; and IVUS lumen and stent area measurements must be accurate. A survey of interventional cardiology fellows reported that independence and preparedness for practice was only 15% in all components of IVUS.[12] Thus, ML model segmentation might be helpful to generalize IVUS quantitative assessment as well as device selection with accuracy to overcome the lack of experience and/or education.

Lastly, the penetration rate of IVUS usage in daily practice is quite different among the regions.[31-34] The reasons for not using IVUS include finances and education.[12] Prior studies demonstrated that IVUS-guided DES implantation is likely to be cost-effective compared with angiography guidance alone.[35,36] In terms of the lack of physician education, IVUS measurements must be accurate in the clinical setting because when an inappropriately large sized balloon or stent is chosen, there is a risk of perforation; or an inappropriately small sized balloon or

TABLE 3 **Prediction of the Errors of Balloon Sizing Using Multivariable Linear Regression Model**

	Regression Coefficient (95% CI)	*P* Value
Myocardial bridge	−0.03 (−0.14 to 0.08)	0.57
Vessel diameter by expert, mm	−0.01 (−0.04 to 0.01)	0.31
Vessel location in LAD	−0.03 (−0.08 to 0.01)	0.14
Vessel visibility >180°	−0.22 (−0.28 to −0.17)	<0.0001

LAD = left anterior descending.

FIGURE 7 **The Difference of Lumen Area Between Expert Analysis and Machine Learning Model Segmentation**

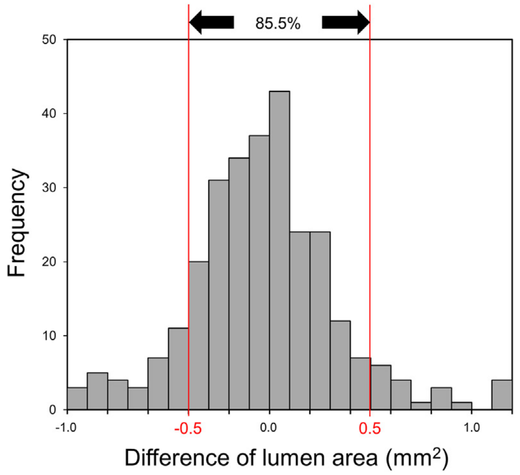

stent is chosen, stent under-expansion is likely and may result in in-stent restenosis or thrombosis. To overcome the above, ML model segmentation can be very helpful for the physician to choose the appropriate balloon size in daily practice.

STUDY LIMITATIONS. First, the ML model was dedicated to just segmentation of lumen, vessel, and stent areas and did not function for qualitative assessment such as detecting dissection, malapposition, percent stent expansion, and calcified or attenuated regions, which would also be important in the clinical setting. Second, a separate test cohort was selected from one site; and it was relatively small, especially for the stent assessment. Multiple sites from around the world need to be tested to establish the ML model further. Third, we included only HD 60 MHz IVUS images; the constructed ML model was therefore not directly applicable to IVUS images obtained with lower frequency ultrasound signals that have a larger area compared to phantoms.[37]

CONCLUSIONS

The ML model IVUS segmentation of lumen, vessel, and stent areas was strongly and positively correlated with those obtained in manually labeled expert analysis. More than 90% of images selected an appropriate balloon size by using both vessel and lumen diameters.

ACKNOWLEDGMENTS The authors thank Dr Takahide Suzuki from Asahikawa-Kosei General Hospital, Dr Masayuki Doi from Kagawa Prefectural Central Hospital, Dr Masanobu Namura from Kanazawa Cardiovascular Hospital, Dr Tatsuya Ito from Nagoya Heart Center, Dr Tadafumi Akimitsu from Oita Cardiovascular Hospital, Dr Hitoshi Anzai from Ota Memorial Hospital, Dr Tadaya Sato from Saka General Hospital, Dr Hiroaki Abe from Takatsuki General Hospital, Dr Shunzo Matsuoka from Uji Tokushukai Medical Center, Dr Hiroki Uehara from Urasoe General Hospital, and Dr Hiroyuki Hikita from Yokosuka Kyosai Hospital for their contribution.

FUNDING SUPPORT AND AUTHOR DISCLOSURES

Dr Matsumura is a consultant for TERUMO Corporation and Boston Scientific Corporation. Dr Mintz has received honoraria from Boston Scientific Corporation. Dr Fall is a consultant for Boston Scientific Corporation, Conavi, and Infraredx. Dr Kirtane received institutional funding to Columbia University and/or Cardiovascular Research Foundation from Medtronic, Boston Scientific, Abbott Vascular, Amgen, CSI, Philips, ReCor Medical, Neurotronic, Biotronik, Chiesi, Bolt Medical, Magenta Medical, Canon, SoniVie, Shockwave Medical, and Merck; in addition to research grants, institutional funding includes fees paid to Columbia University and/or Cardiovascular Research Foundation for consulting and/or speaking engagements in which Dr Kirtane controlled the content; and he received personal consulting fees from IMDS; and travel expenses/meals from Medtronic, Boston Scientific, Abbott Vascular, CSI, Siemens, Philips, ReCor Medical, Chiesi, OpSens, Zoll, and Regeneron. Dr Maehara is a consultant for Boston Scientific and Shockwave; and on the advisory board for SepctraWave. All other authors have reported that they have no relationships relevant to the contents of this paper to disclose.

ADDRESS FOR CORRESPONDENCE: Dr Akiko Maehara, Columbia University Medical Center, Cardiovascular Research Foundation, 1700 Broadway, 9th Floor, New York, New York 10019, USA. E-mail: amaehara@crf.org.

PERSPECTIVES

COMPETENCY IN MEDICAL KNOWLEDGE: During PCI, IVUS informs appropriate device sizing and good stent expansion to the operators to improve patient outcomes in both short- and long-term follow-up studies compared with angiography alone.

TRANSLATIONAL OUTLOOK: Correlation between ML and experts' lumen and vessel area measurements were excellent. The agreement rates between ML and experts' measurements for both appropriate balloon size selection and lumen measurements were about 90%. Extend ML to identify calcified or attenuated plaques which impact lesion preparation and post-PCI outcomes.

REFERENCES

1. Maehara A, Matsumura M, Ali ZA, Mintz GS, Stone GW. IVUS-guided versus OCT-guided coronary stent implantation: a critical appraisal. *J Am Coll Cardiol Img*. 2017;10:1487–1503.

2. Mintz GS, Matsumura M, Ali Z, Maehara A. Clinical utility of intravascular imaging: past, present, and future. *J Am Coll Cardiol Img*. 2022;15(10):1799–1820.

3. Maehara A, Mintz GS, Wintzenbichler B, et al. Relationship between intravascular ultrasound guidance and clinical outcomes after drug-eluting stents. *Circ Cardiovasc Interv*. 2018;11:e006243.

4. Hong SJ, Kim BK, Shin DH, et al. Effect of intravascular ultrasound-guided vs angiography-guided everolimus-eluting stent implantation the IVUS-XPL randomized clinical trial. *JAMA*. 2015;314(20):2155–2163.

5. Zhang J, Gao X, Kan J, et al. Intravascular ultrasound versus angiography-guided drug-eluting stent implantation: the ULTIMATE trial. *J Am Coll Cardiol*. 2018;72:3126–3137.

6. Gao XF, Ge Z, Kong XQ, et al. 3-Year outcomes of the ULTIMATE trial comparing intravascular ultrasound versus angiography-guided drug-eluting stent implantation. *J Am Coll Cardiol Intv*. 2021;14:247–257.

7. Hong SJ, Mintz GS, Ahn CM, et al. Effect of intravascular ultrasound-guided drug-eluting stent implantation: 5-year follow-up of the IVUS-XPL randomized trial. *J Am Coll Cardiol Intv*. 2020;13:62–71.

8. Lawton JS, Tamis-Holland JE, Bangalore S, et al. 2021 ACC/AHA/SCAI guideline for coronary artery revascularization: executive summary: a report of the American College of Cardiology/American Heart Association joint committee on clinical practice guidelines. *J Am Coll Cardiol*. 2022;79:e21–e129.

9. Raber L, Mintz GS, Koskinas KC, et al. Clinical use of intracoronary imaging. Part 1: guidance and optimization of coronary interventions. An expert consensus document of the European Association of Percutaneous Cardiovascular Interventions. *Eur Heart J*. 2018;39:3281–3300.

10. Smilowitz NR, Mohananey D, Razzouk L, Weisz G, Slater JN. Impact and trends of intravascular imaging in diagnostic coronary angiography and percutaneous coronary intervention in inpatients in the United States. *Catheter Cardiovasc Interv*. 2018;92:E410–E415.

11. Mentias A, Sarrazin MV, Saad M, et al. Long-term outcomes of coronary stenting with and without use of intravascular ultrasound. *J Am Coll Cardiol Intv*. 2020;13:1880–1890.

12. Flattery E, Rahim HM, Petrossian G, et al. Competency-based assessment of interventional cardiology fellows' abilities in intracoronary physiology and imaging. *Circ Cardiovasc Interv*. 2020;13:e008760.

13. Balakrishna C, Dadashzadeh S, Soltaninejad S. Automatic detection of lumen and media in the IVUS images using U-Net with VGG16 encoder. *arXiv*. 2018. https://doi.org/10.48550/arXiv.1806.07554

14. Fedewa R, Puri R, Fleischman E, et al. Artificial intelligence in intracoronary imaging. *Curr Cardiol Rep*. 2020;22:46.

15. Yang J, Faraji M, Basu A. Robust segmentation of arterial walls in intravascular ultrasound images using dual path U-Net. *Ultrasonics*. 2019;96:24–33.

16. Ronneberger O, Fischer P, Brox T. U-Net: convolutional networks for biomedical image segmentation. *arXiv*. 2015. https://doi.org/10.48550/arXiv.1505.04597

17. Yang J, Tong L, Faraji M, Basu A. IVUS-Net: an intravascular ultrasound segmentation network. *arXiv*. 2018. https://doi.org/10.48550/arXiv.1806.03583

18. Ali ZA, Maehara A, Genereux P, et al. Optical coherence tomography compared with intravascular ultrasound and with angiography to guide coronary stent implantation (ILUMIEN III: OPTIMIZE PCI): a randomised controlled trial. *Lancet*. 2016;26(388):2618–2628.

19. Gerbaud E, Weisz G, Tanaka A, et al. Multi-laboratory inter-institute reproducibility study of IVOCT and IVUS assessments using published consensus document definitions. *Eur Heart J Cardiovasc Imaging*. 2016;17:756–764.

20. de Jaegere P, Mudra H, Figulla H, et al. Intravascular ultrasound-guided optimized stent deployment. Immediate and 6 months clinical and angiographic results from the Multicenter Ultrasound Stenting in Coronaries Study (MUSIC Study). *Eur Heart J*. 1998;19:1214–1223.

21. Unal G, Bucher S, Carlier S, et al. Shape-driven segmentation of the arterial wall in intravascular ultrasound images. *IEEE Trans Inf Technol Biomed*. 2008;12:335–347.

22. Mendizabai-Ruiz G, Rivera M, Kakadiaris A. Segmentation of the luminal border in intravascular ultrasound B-mode images using a probabilistic approach. *Med Image Anal*. 2013;17:649–670.

23. Nishi T, Yamashita R, Imura S, et al. Deep learning-based intravascular ultrasound segmentation for the assessment of coronary artery disease. *Int J Cardiol*. 2021;333:55–59.

24. Chieffo A, Latib A, Caussin C, et al. A prospective, randomized trial of intravascular-ultrasound guided compared to angiography guided stent implantation in complex coronary lesions: the AVIO trial. *Am Heart J*. 2013;165:65–72.

25. Gary SM, Kent KM, Pichard AD, et al. Contribution of inadequate arterial remodeling to the development of focal coronary artery stenoses. *Circulation*. 1997;95:1791–1798.

26. Song HG, Kang SJ, Ahn JM, et al. Intravascular ultrasound assessment of optimal stent area to prevent in-stent restenosis after zotarolimus-, everolimus-, and sirolimus-eluting stent implantation. *Catheter Cardiovasc Interv*. 2014;83:873–878.

27. Lee SY, Shin DH, Kim JS, et al. Intravascular ultrasound predictors of major adverse cardiovascular events after implantation of everolimus-eluting stents for long coronary lesions. *Rev Esp Cardiol (Engl Ed)*. 2017;70:88–95.

28. Katagiri Y, De Maria GL, Kogame N, et al. Impact of post-procedural minimal stent area on 2-year clinical outcomes in the SYNTAX II trial. *Catheter Cardiovasc Interv*. 2019;93:E225–E234.

29. Kumar A, Shariff M, Adalja D, et al. Intravascular ultrasound versus angiogram guided drug eluting stent implantation. A systematic review and updated meta-analysis with trial sequential analysis. *Int J Cardiol Heart Vasc*. 2019;25:100419.

30. Zhang Y, Farooq V, Garcia-Garcia HM, et al. Comparison of intravascular ultrasound versus angiography-guided drug-eluting stent implantation: a meta-analysis of one randomised trial and ten observational studies involving 19,619 patients. *EuroIntervention*. 2012;8:855–865.

31. Bergmark BA, Osborn EA, Ali ZA, et al. Association between intracoronary imaging during PCI and clinical outcomes in a real-world US medicare population. *Journal of the Society for Cardiovascular Angiography & Interventions*. 2023;2:100556.

32. Jones DA, Rathod KS, Koganti S, et al. Angiography alone versus angiography plus optical coherence tomography to guide percutaneous coronary intervention: outcomes from the pan-london PCI cohort. *J Am Coll Cardiol Intv*. 2018;11:1313–1321.

33. Shin DH, Kang HJ, Jang JS, et al. The current status of percutaneous coronary intervention in Korea: based on year 2014 & 2016 cohort of Korean percutaneous coronary intervention (K-PCI) registry. *Korean Circ J*. 2019;49:1136–1151.

34. Kuno T, Numasawa Y, Sawano M, et al. Real-world use of intravascular ultrasound in Japan: a report from contemporary multicenter PCI registry. *Heart Ves*. 2019;34:1728–1739.

35. Zhou J, Liew D, Shaw J, et al. Intravascular ultrasound versus angiography-guided drug-eluting stent implantation; a health economic analysis. *Circ Cardiovasc Qual Outcomes*. 2021;14:e006789.

36. Alberti A, Giudice P, Gelera A, et al. Understanding the economic impact of intravascular ultrasound (IVUS). *Eur J Health Econ*. 2016;17:185–193.

37. Kubo T, Akasaka T, Shite J, et al. OCT compared with IVUS in a coronary lesion assessment: the OPUS-CLASS study. *J Am Coll Cardiol Img*. 2013;6:1095–1104.

KEY WORDS balloon sizing, convolution neural network, coronary artery, high-definition intravascular ultrasound, machine learning

APPENDIX For supplemental tables and figures, please see the online version of this paper.